PRAMANA
— journal of
physics

Vol. 86, No. 5
May 2016
pp. 1021–1030

Delay signatures in the chaotic intensity output of a quantum dot laser with optical feedback

BEJOY VARGHESE[1,*], MANU P JOHN[2] and V M NANDAKUMARAN[1,3]

[1]International School of Photonics, Cochin University of Science and Technology, Kochi 682 022, India
[2]Department of Physics, Union Christian College, Aluva 683 102, India
[3]Department of Physics, Amrita School of Arts and Sciences, Amrita Viswa Vidyapeetham, Kollam 690 525, India
*Corresponding author. E-mail: bejoyrosily@gmail.com

MS received 23 February 2015; revised 20 May 2015; accepted 1 June 2015
DOI: 10.1007/s12043-016-1193-y; ***e*Publication:** 15 February 2016

Abstract. Delay identification from the chaotic intensity output of a quantum dot laser with optical feedback is done using numerical and information theoretic techniques. Four quantifiers, namely autocorrelation function, delayed mutual information, permutation entropy and permutation statistical complexity, are employed in delay estimation. A detailed comparison of these quantifiers with different feedback rates and delay is undertaken. Permutation entropy and permutation statistical complexity are calculated with different dimensions of symbolic reconstruction to obtain the best results.

Keywords. Quantum dot laser; delay; information entropy; statistical complexity; mutual information.

PACS No. 05.10.−a

1. Introduction

Research in complex systems require quantitative predictions of their dynamics, even before we completely understand the underlying mechanisms. This can only be done by collecting data about the past evolution and retrieving the structures in the dynamics from the collected data. Numerous statistical and information theoretic approaches have been successfully employed for analysing the time series obtained from the observation of complex processes. Due to the finite speed of information propagation, interaction between different components of a complex system does inevitably involve time delays. Identifying these delays is crucial for modelling and forecasting applications in different fields including biology [1], optics [2,3] and climate science [4]. The most conventional and widely used methods for estimating delay in complex dynamics are autocorrelation function (ACF) and delayed mutual information (DMI). Several new techniques were recently

discovered for delay identification. Information theory measures like entropy and complexity have been shown to be particularly useful in the case of nonlinear systems [3,5]. In the present work, we focus on the dynamics of a quantum dot laser (QDL) with optical feedback working in the coherence collapse regime. Dynamics of QDLs show quite distinctive features compared to bulk semiconductor dynamics. Conventional Lang–Kobayashi equations fail in many instances to accurately predict QDL dynamics [6]. In QDLs, relaxation oscillations are strongly damped due to different carrier capture dynamics into the quantum dots (QDs) [7]. Strong damping along with relatively small linewidth enhancement factor (α) make QDLs less sensitive to optical feedback [8]. So instabilities in QDLs occur at higher feedback strengths compared to bulk or quantum well (QW) lasers. Synchronization of QDLs working in the chaotic regime is currently an active research area with the prospect of using them for secure communication with chaotic carriers [9]. A major concern in chaos-based secure communication is the level of difficulty to identify the parameters of the chaotic emitter from the output time series. Chaos generated in feedback systems can have very high dimensionality due to the infinite number of degrees of freedom introduced by time delay. But once the delay value is retrieved from the time series, the high-dimensional attractor can be projected to a low-dimensional phase space, which may result in low-complexity numerical techniques to decrypt the information. This security aspect of chaos-based communication had been addressed for semiconductor lasers modelled with conventional Lang–Kobayashi equations [3,10,11]. Rontani *et al* [10] showed that a careful choice of laser operating conditions can make delay retrieval extremely difficult. In another work [11], the same group also demonstrated that the time-scales of laser dynamics in its route to chaos, influence the difficulty in delay identification. Recently, information theory measures like permutation entropy (H_S) and permutation statistical complexity (C_{JS}) were employed to get good estimates of delay value from the time series of delay differential systems. Soriano *et al* [3] used this approach to find intrinsic time-scales in the dynamics of a semiconductor laser with optical feedback operating in the coherence collapse regime. We use ACF, DMI, H_S and C_{JS} to retrieve delay from the chaotic output intensity series of a QDL with external cavity. Reliability of these measures is investigated when external cavity round trip time and feedback rates are varied.

2. Theoretical framework

2.1 *Rate equation model*

We adopt the dynamical model of QDL from ref. [8]. This model presumes that the carriers are first injected into the quantum well before being captured into the quantum dots. The dynamics is described by the following set of delay differential equations that give time evolution of the complex amplitude of the electric field (E), occupation probability in a dot (ρ) and the carrier density in the well (N).

$$\dot{E} = -\frac{E}{2\tau_s} + \frac{g_0 V}{2}(2\rho - 1)E + i\frac{\delta\omega}{2}E + \frac{\gamma}{2}E(t-\tau), \tag{1}$$

$$\dot{\rho} = -\frac{\rho}{\tau_d} - g_0(2\rho - 1)|E|^2 + F(N,\rho), \tag{2}$$

$$\dot{N} = \frac{J}{q} - \frac{N}{\tau_n} - 2N_{\mathrm{d}}F(N, \rho). \tag{3}$$

τ_s, τ_n and τ_d are the photon lifetime, carrier lifetime in the well and the carrier lifetime in the dot, respectively. $g_0 = \sigma v_{\mathrm{g}}$, where σ is the cross-section of interaction of the carriers in the dots with the electric field and v_{g} is the group velocity. $V = 2N_{\mathrm{d}}\Gamma/d$, where N_{d} is the two-dimensional density of dots, Γ is the confinement factor and d is the thickness of the dot layer. γ is the feedback rate and τ is the delay involved in the feedback process. $F(N, \rho)$ is the rate of exchange of carriers between the well and the dots and is given by $F(N, \rho) = R_{\mathrm{cap}}(1 - \rho) - R_{\mathrm{esc}}\rho$. $R_{\mathrm{cap}} = CN^2 + BN$, where B describes carrier–phonon capture and C describes Auger carrier capture. For simulations, B is taken as zero. This is justified because discrete nature of QD energy levels and fixed energies of longitudinal optical (LO) phonons make carrier–phonon capture in QD structures highly improbable [7]. Temperature-dependent carrier escape from the dots is given by R_{esc}. $\delta\omega$ takes into account the dependence of laser frequency on carrier densities in QW and QD regions. $\delta\omega = \beta_1 N + \beta_2\rho$ where plasma effect from the carriers in the well is described by β_1 and variations caused by population in the dots is described by β_2 [8]. The values used in the simulations are $\tau_s = 3$ ps, $\tau_n = \tau_d = 1$ ns, $g_0 = 0.9259 \times 10^{-10}\,\mathrm{m^3\,s^{-1}}$, $V = 2.4 \times 10^{22}\,\mathrm{m^{-3}}$, $N_{\mathrm{d}} = 2 \times 10^{15}\,\mathrm{m^{-2}}$, $\beta_1 = 0$, $\beta_2 = 2$, $C = 10^{-20}\,\mathrm{m^4\,s^{-1}}$, $R_{\mathrm{esc}} = 0$ [8].

2.2 *Autocorrelation function*

ACF quantifies the linear relationship between a signal and its time-shifted version. ACF for a random process $X(t)$ is defined as

$$\Gamma(\theta) = \frac{1}{\hat{\sigma}_X^2}\langle (x(t) - \hat{\mu}_X)(x(t+\theta) - \hat{\mu}_X)\rangle, \tag{4}$$

where $x(t)$ and $x(t + \theta)$ are sampled from $X(t)$. $\hat{\mu}_X = \langle x(t)\rangle$ and $\hat{\sigma}_X = \langle (x(t) - \hat{\mu}_X)^2\rangle^{1/2}$. $\langle\cdot\rangle$ denotes expectation value.

2.3 *Permutation entropy*

One of the natural approaches to quantify the information content of a process is the Shannon entropy (H). H is calculated from a probability distribution $P = \{p_i : i = 1, ..., M\}$ of some observable, associated with the process. M represents the total number of states the observable can take.

$$H[P] = -\sum_{i=1}^{M} p_i \ln(p_i). \tag{5}$$

It is also the measure of uncertainty associated with the process. If we can perfectly predict the outcome at any instant, there is minimum uncertainty, and $H[P] = 0$. In contrast, if there is equal probability for all the states to occur, uncertainty is maximum and $H[P_e] = \ln(M)$. Here P_e denotes uniform probability distribution and $P_e = \{1/M, 1/M, ..., 1/M\}$. To find the associated probability distribution, we use Bandt and Pompe symbolization method, which has recently been applied successfully in the time series analysis of chaotic dynamical systems. A detailed description of the method is

given in refs [3] and [5]. The method is briefly explained below. Given a time series $x_t, t = 1, 2, ..., n$, an embedding dimension D and a time delay (τ), a D-dimensional vector is constructed as

$$s \mapsto (x_{s-(D-1)\tau}, x_{s-(D-2)\tau}, ..., x_{s-\tau}, x_s). \tag{6}$$

This vector is then rearranged as

$$x_{s-r_0\tau} \geq x_{s-r_1\tau} \geq x_{s-r_2\tau} \geq \cdots \geq x_{s-r_{D-2}\tau} \geq x_{s-r_{D-1}\tau}, \tag{7}$$

to get an ordinal pattern

$$\pi = (r_0, r_1, ..., r_{D-1}). \tag{8}$$

Each possible ordinal pattern that is generated in this way, is an element of the set of all permutations of $(0, 1, ..., D-1)$. If we have a sufficiently long time series that satisfy $N \gg D!$, an ordinal pattern probability distribution $P = \{p(\pi_i), i = 1, 2, ..., D!\}$ can be generated. Shannon entropy calculated using this probability distribution is the permutation entropy denoted by H_S. In the following discussions, permutation entropy is always used in the normalized form given by

$$H_S[P] = H[P]/H[P_e]. \tag{9}$$

2.4 *Delayed mutual information*

Mutual information of two discrete random variables X and Y, is defined as [10,11]

$$I(X, Y) = \sum_{x\in X} \sum_{y\in Y} p(x, y) \log\left(\frac{p(x, y)}{p(x)p(y)}\right), \tag{10}$$

where $p(x)$ and $p(y)$ are marginal probability density functions and $p(x, y)$ is the joint probability density function. DMI can also be defined in terms of H

$$I(\theta) = H(X(t)) + H(X(t+\theta)) - H(X(t), X(t+\theta)). \tag{11}$$

DMI between $X(t)$ and $X(t+\theta)$ can be obtained from the first definition as

$$I(\theta) = \sum_{x, x(t+\theta)\in X} p(x(t), x(t+\theta)) \log\left(\frac{p(x(t), x(t+\theta))}{p(x(t))p(x(t+\theta))}\right). \tag{12}$$

2.5 *Permutation statistical complexity*

Statistical complexity measures can provide useful information about the structure of the underlying dynamics when the dynamics is not perfectly random or ordered [12]. So, by definition, statistical complexity goes to zero as the process tend to either of these extremes [13,14]. Permutation statistical complexity (C_{JS}) is defined over two

probability distributions – probability distribution of the ordinal patterns (P) obtained as discussed previously and the uniform distribution (P_e).

$$C_{JS}[P] = Q_J[P, P_e]H_S[P], \tag{13}$$

where Q_J is the disequilibrium which quantifies how distant P is from P_e. Q increases if the system has preferred states among the accessible ones. Q_J is defined in terms of Jensen–Shannon divergence $\mathscr{J}[P, P_e]$.

$$Q_J[P, P_e] = Q_0 \mathscr{J}[P, P_e] \tag{14}$$

with

$$\mathscr{J}[P, P_e] = H[[P + P_e]/2] - H[P]/2 - H[P_e]/2. \tag{15}$$

Q_0 is a normalization constant corresponding to the maximum possible value of $\mathscr{J}[P, P_e]$ which is equal to $-2\{((N+1)/2)\ln(N+1) - 2\ln(2N) + \ln N\}^{-1}$. Maximum value for $\mathscr{J}[P, P_e]$ occurs for a distribution P, which has a particular component (p_j) equal to 1, and all the remaining components are zero.

3. Numerical simulations

Dynamical equations are scaled properly before performing numerical calculations. Time (t) is nondimensionalized by scaling it with respect to the photon lifetime as $t/2\tau_s$. Feedback rate (γ) and electric field (E) are scaled as $\tau_s\gamma$ and $(2\tau_s g_0)^{-1/2}E$, respectively. Simulations are done using second-order Runge–Kutta method and the output is sampled with a period $\Delta_s = 0.01$. 2×10^8 points are used for the calculations. Figure 1 shows the graph of the four quantifiers discussed in previous sections for $\gamma = 0.18$ and $\tau = 66.66$. This delay value corresponds to 400 ps in the original time-scale. Relaxation oscillation period is approximately 89 ps which scales to $\tau_{RO} \approx 14.83$. Figure 1a shows ACF as a function of the shift in time series. ACF does not have any vividly indicative feature near the value of τ, from which one can estimate the time delay involved in the feedback process. In contrast to ACF, the other three quantifiers give an affirmative indication of the delay. For highly nonlinear systems like QDL with optical feedback, it is necessary to detect the nonlinear nonlocal time correlations in the output intensity series if one wants to estimate the inherent delay in the time evolution of state variables. The ambiguity in delay estimation from ACF is attributed to the fact that it detects only linear correlations [11]. Figure 1b plots DMI with the inset graph showing the enlarged portion near the delay value. There is a pronounced peak near τ, which is slightly shifted to the right. This shift originates from the finite response time of the laser. The prediction of the response time beforehand is difficult and is an inherent property of the laser. Two less dominant peaks appear on both sides of the delay peak at $\tau \pm \tau_{RO}/2$. In the figure, the peak on the higher side of τ is more dominant than that on the lower side. The height of the delay peak as well as of the sidebands depends on the value of γ. This dependence is discussed later in this section. Figures 1c and 1e show the plots obtained for H_S and C_{JS} for D from 5 to 9. When the dynamics is reconstructed with a proper value of delay, a minimum in entropy and a maximum in complexity are expected. Figure 1c shows the plot of both the measures together. The more pronounced C_{JS} peak is visible in this plot,

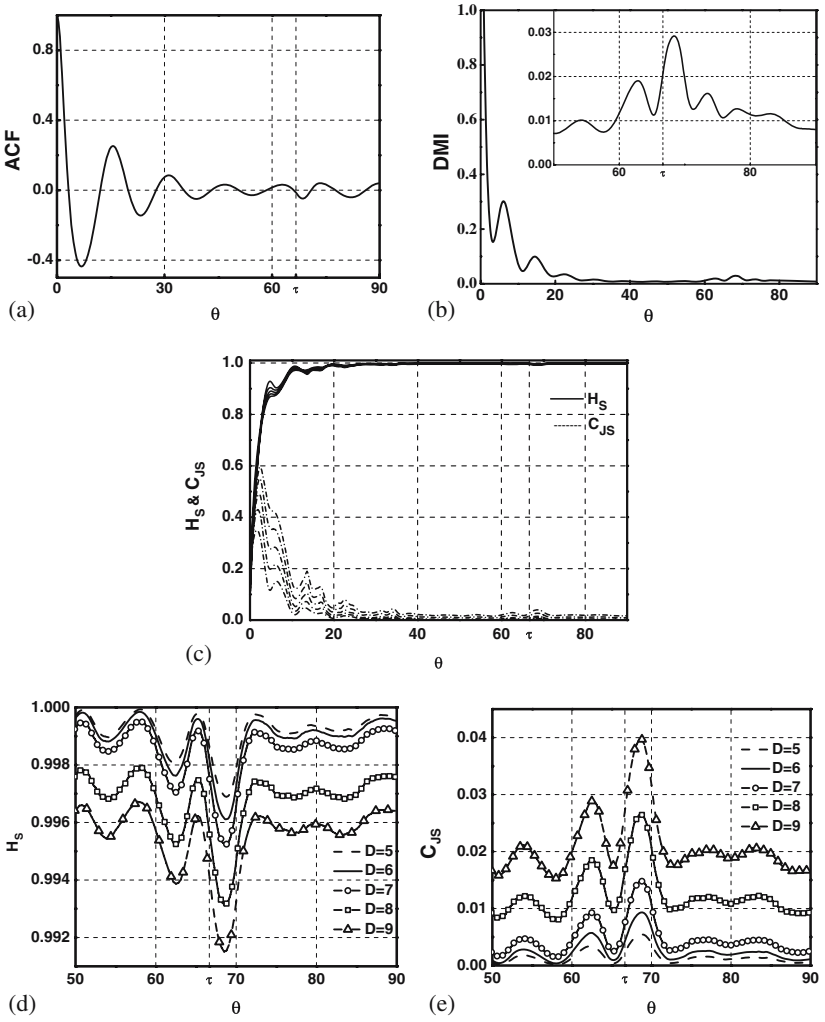

Figure 1. (**a**) ACF, (**b**) DMI, (**c**) H_S and C_{JS} calculated from the output intensity time series of QDL for $\tau = 400$ ps and $\gamma = 0.18$. For H_S and C_{JS}, D is varied from 5 to 9. (**d**) and (**e**) show enlarged parts of H_S and C_{JS} respectively, near the value of τ.

but it is difficult to spot the dip in H_S as its contrast from the baseline is low. The dip in H_S and the peak in C_{JS} near $\theta = \tau$ is evident from the enlarged graphs in figures 1d and 1e. Like DMI, delay estimations from both these measures suffer from the finite response time of the laser. Shift in the peak(dip) from the actual value of delay is found to be the same in all the three cases. In the complexity and entropy plots, the peak(dip) at $\tau + \tau_{RO}/2$ is suppressed, while the one at $\tau - \tau_{RO}/2$ is visible. As the dimensionality of reconstruction increases, the delay signature becomes prominent in both H_S and C_{JS}. But increasing D to 10 gives a different result. In figure 2 entropy and complexity are plotted for $D = 9$ and 10. For $D = 10$, H_S increases for all values of θ reducing the contrast of the dip near τ. But C_{JS} peaks near $\theta = \tau'$ and $\tau' - \tau_{RO}'/2$ are enhanced.

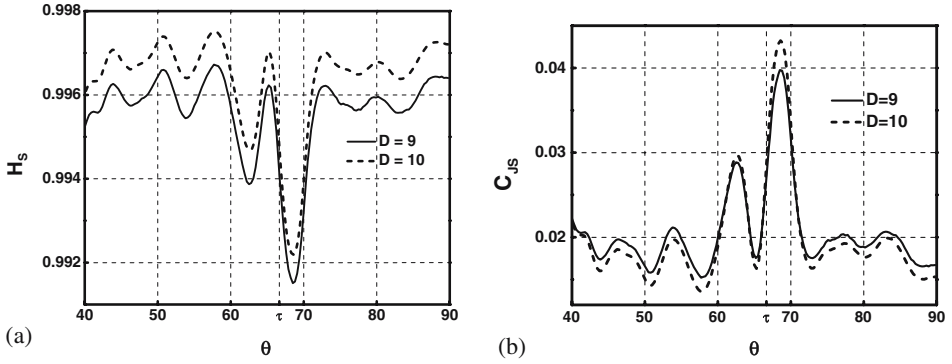

Figure 2. (**a**) H_S and (**b**) C_{JS} for $D = 9$ and 10. $\tau = 400$ ps and $\gamma = 0.18$.

Interestingly, for other values of θ, $C_{JS}[D = 10]$ is less than $C_{JS}[D = 9]$. This shows that better delay retrieval using higher values of D is possible if one uses C_{JS}, even when H_S fails to give an estimation. For higher values of D, we get better contrast for the delay peak because the values of complexity in the background get considerably reduced. Next we perform the same calculations for $\tau \approx 33.33$ (200 ps) by keeping all other parameters constant. The results are given in figure 3. H_S and C_{JS} are plotted only for $D = 9$. Even

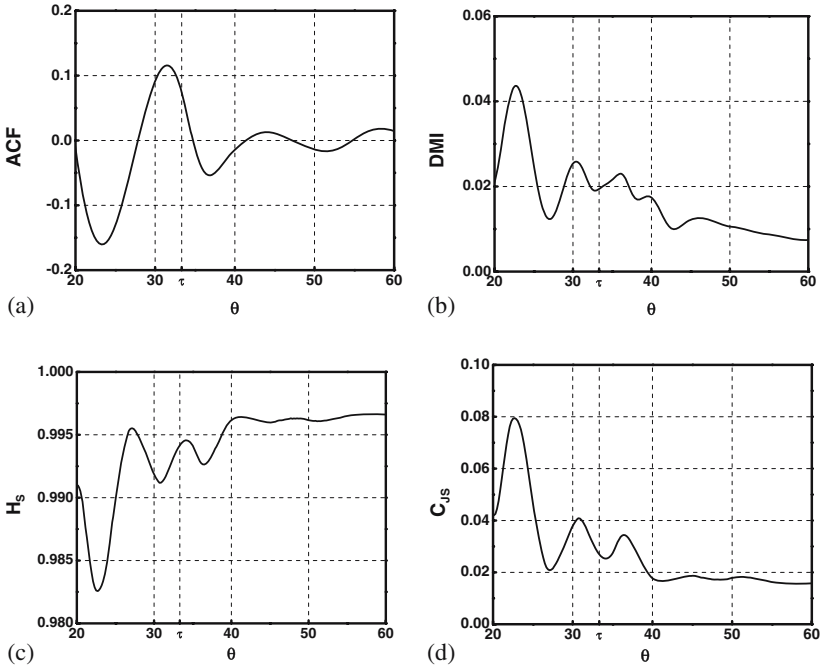

Figure 3. (**a**) ACF, (**b**) DMI, (**c**) H_S and (**d**) C_{JS} calculated from output intensity time series of QDL for $\tau = 33.33$ (200 ps) and $\gamma = 0.18$. $D = 9$ for H_S and C_{JS}.

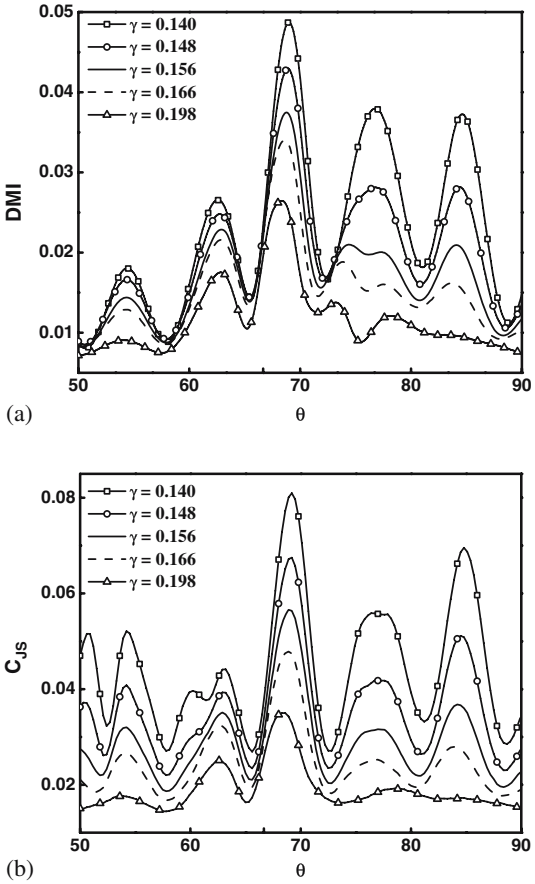

Figure 4. (**a**) DMI and (**b**) C_{JS} calculated for six different values of feedback rate (γ) with $\tau = 66.66$ (400 ps).

by a closer scrutiny, no affirmative feature indicative of delay can be spotted in any of the four plots. This reveals the practical impossibility of delay identification when the actual delay gets closer to the relaxation oscillation period. Numerous correlations exist in the QDL dynamics which die only long after the value of θ exceeds the value of τ. So when the delay gets closer to the relaxation oscillation period, the delay signature gets immersed in these correlations and a proper estimation becomes impossible. Finally, we study the behaviour of DMI and C_{JS} when feedback rate is varied. Figures 4a and 4b show these quantifiers for six different values of γ. Delay is set to 66.66 (400 ps) in all the cases and the feedback rates are chosen such that the dynamics is chaotic. For both DMI and C_{JS}, higher peaks are obtained for lower values of γ. In the figure, highest peak is obtained for $\gamma = 0.14$. But due to the pronounced peaks at $\tau \pm \tau_{RO}/2$, delay estimation can become ambiguous. As feedback rate increases, the delay peaks reduce height but as the nearby peaks diminish faster, contrast from the baseline gets enhanced. Especially for C_{JS}, peaks at $\theta > \tau$ get flattened. When feedback rate is high, the delay estimation

become more accurate because the shift due to the finite laser response time reduces and the peaks get closer to the actual value of the delay. This happens identically for both DMI and C_{JS}.

4. Conclusions

We investigate the delay estimation scenarios from the chaotic time series using four quantifiers – namely autocorrelation function, delayed mutual information, permutation entropy and permutation statistical complexity. These numerical and information theoretical techniques are applied to the chaotic output intensity of a quantum dot laser with optical feedback. A detailed comparison of these measures is performed for different feedback rates and delays. From the numerical calculations performed, we find permutation statistical complexity to be the best candidate due to its distinctive maximum close to the delay. Also, we show that higher dimensionality of symbolic reconstruction will work with permutation statistical complexity to get better contrast against the background as opposed to permutation entropy. Autocorrelation function fails to give a distinctive identification unlike the other three measures. When the delay involved in feedback is close to the relaxation oscillation period of the laser, delay identification becomes practically impossible with any of these techniques. Due to the finite laser response time all the measures have an error which gives a slightly higher estimation of delay. For high feedback rates, delay estimations become more accurate because the shift due to finite laser response reduces.

Acknowledgements

Authors thank BRNS for its financial support.

References

[1] M C Mackey and L Glass, *Science* **197(4300)**, 287 (1977), http://www.sciencemag.org/content/197/4300/287.full.pdf, http://www.sciencemag.org/content/197/4300/287.abstract

[2] Christian Otto, Kathy Lüdge and Eckehard Schöll, *Phys. Status Solidi* **247(4)**, 829 (2010), doi:10.1002/pssb.200945434

[3] M C Soriano, L Zunino, O A Rosso, Ingo Fischer and C R Mirasso, *IEEE J. Quantum Electron.* **47(2)**, 252 (2011)

[4] Eli Tziperman, Lewi Stone, Mark A Cane and Hans Jarosh, *Science* **264(5155)**, 72 (1994), http://www.sciencemag.org/content/264/5155/72.full.pdf, http://www.sciencemag.org/content/264/5155/72.abstract

[5] L Zunino, M C Soriano, I Fischer, O A Rosso and C R Mirasso, *Phys. Rev. E* **82**, 046212 (2010), http://link.aps.org/doi/10.1103/PhysRevE.82.046212

[6] Amin H Al-Khursan, Basim Abdullattif Ghalib and Sabri J Al-Obaidi, *Semiconductors* **46(2)**, 213 (2012), doi:10.1134/S1063782612020029

[7] A V Uskov, Y Boucher, J Le Bihan and J McInerney, *Appl. Phys. Lett.* **73(11)**, 1499 (1998), http://scitation.aip.org/content/aip/journal/apl/73/11/10.1063/1.122185

[8] D O'Brien, S P Hegarty, G Huyet and A V Uskov, *Opt. Lett.* **29(10)**, 1072 (2004), http://ol.osa.org/abstract.cfm?URI=ol-29-10-1072

[9] Basim Abdullattif Ghalib, Sabri J Al-Obaidi and Amin H Al-Khursan, *Opt. Laser Technol.* **48**, 453 (2013), http://www.sciencedirect.com/science/article/pii/S0030399212005385
[10] D Rontani, A Locquet, M Sciamanna and D S Citrin, *Opt. Lett.* **32(20)**, 2960 (2007), http://ol.osa.org/abstract.cfm?URI=ol-32-20-2960
[11] D Rontani, A Locquet, M Sciamanna, D S Citrin and S Ortin, *IEEE J. Quantum Electron.* **45(7)**, 879 (2009)
[12] M T Martin, A Plastino and O A Rosso, *Physica A* **369(2)**, 439 (2006), http://www.sciencedirect.com/science/article/pii/S0378437106001324
[13] B A Huberman and T Hogg, *Phys. D* **2(1–3)**, 376 (1986), http://dl.acm.org/citation.cfm?id=25201.25226
[14] M T Martin, A Plastino and O A Rosso, *Phys. Lett. A* **311(23)**, 126 (2003), http://www.sciencedirect.com/science/article/pii/S0375960103004912